Primordial Black Hole Review
LISA CosWG project 11

10th LISA CosWG Meeting, Stavanger, 6 June 2023

Juan García-Bellido
IFT-UAM/CSIC Madrid

LISA CONSORTIUM

Campus Internacional excelencia UAM CSIC+

Primordial Black Hole Review

LISA Cos WG Project 11

Originally Proposed: 12th Jun 2018

Officially Started: 24th Sep 2019

Officially Finished: 6th Jun 2023

20 contributors

155 pages

806 references

Journal: Living Reviews Relativity

(Still under LISA internal review)

Primordial Black Hole Review

Primordial black holes and their gravitational-wave signatures

Sebastien Clesse,[a] Juan García-Bellido,[b] Eleni Bagui,[a] Valerio De Luca,[c] Gabriele Franciolini,[d,e] Cristian Joana,[f,g] Rajeev Kumar Jain,[p] Sachiko Kuroyanagi,[b] Ilia Musco,[d,e] Theodoros Papanikolaou,[n,i] Marco Peloso,[r] Alvise Raccanelli,[s1,s2,s3,s4] Sébastien Renaux-Petel,[p] Antonio Riotto,[z] Ester Ruiz Morales,[b,h] Marco Scalisi,[k] Olga Sergijenko,[q] Caner Unal,[l,m,s] Vincent Vennin,[r,i] David Wands[j]

Primordial Black Hole Review

Abstract. In the recent years, primordial black holes (PBHs) have emerged as one of the most interesting and hotly debated topics in cosmology. Among other possibilities, PBHs could explain both some of the signals from binary black hole mergers observed in gravitational wave detectors and an important component of the dark matter in the Universe. Significant progress has been achieved both on the theory side and from the point of view of observations, including new models and more accurate calculations of PBH formation, evolution, clustering, merger rates, as well as new astrophysical and cosmological probes. In this work, we review, analyse and combine the latest developments in order to perform end-to-end calculations of the various gravitational wave signatures of PBHs. Different ways to distinguish PBHs from stellar black holes are emphasized. Finally, we discuss their detectability with LISA, the first planned gravitational-wave observatory in space.

Primordial Black Hole Review

Contents

The goal of this paper is to review these most recent developments and discuss how they impact the GW signatures of PBHs. Compared to other recent reviews, we aim at integrating together the most recent and accurate models, e.g., of PBH formation, evolution, clustering, merger rates, in order to compute the GW signatures of PBHs, and to explore their detectability. For this purpose, we have developed in parallel a numerical code that implements all those models and recent scenarios. The code will be released soon in a separate publication, but it has been already used in this paper in order to produce the key figures. The task of including these increasingly complex models has been eased by the specific expertise of many authors, who have actively contributed to these developments, covering a broad range of topics.

Primordial Black Hole Review

1.3 Probing PBHs with LISA

This project is hosted by the cosmology working group of the LISA consortium. Therefore our discussion has been focused on the GW signatures of PBHs in the particular context of the LISA mission.

PBHs cover a very wide range of masses and therefore frequency ranges of GWs. In particular, LISA will be sensitive to a broad band around the millihertz GW frequencies [125, 144–146], which is complementary to the ground-based GW detectors [90, 91] and electromagnetic probes [147]. The search for a SGWB from PBH formation in the radiation era can be indirectly used for their discovery or alternatively to constrain their existence in the $10^{-12}\ M_\odot$ mass range [125, 144–146, 148]. Moreover, the coalescence of the heavy seeds of supermassive black holes (SMBH) in the late Universe could leave clear signatures of their primordial origin, or even detect individual events at high redshift which could not have arisen from astrophysical mechanisms.

The great sensitivity of LISA at mHz frequencies [149–152] opens the possibility to detect the mergers of $10^3 - 10^4\ M_\odot$ PBHs all the way to $z \simeq 100$. Furthermore, the isotropic SGWB from the coalescence of PBHs since recombination should have an amplitude and spectral shape that will make it easily detectable by LISA. In this review, we will describe the different features of known PBH scenarios that can be probed with LISA.

Primordial Black Hole Review

Primordial Black Hole Review

2.1 Single-field inflationary models

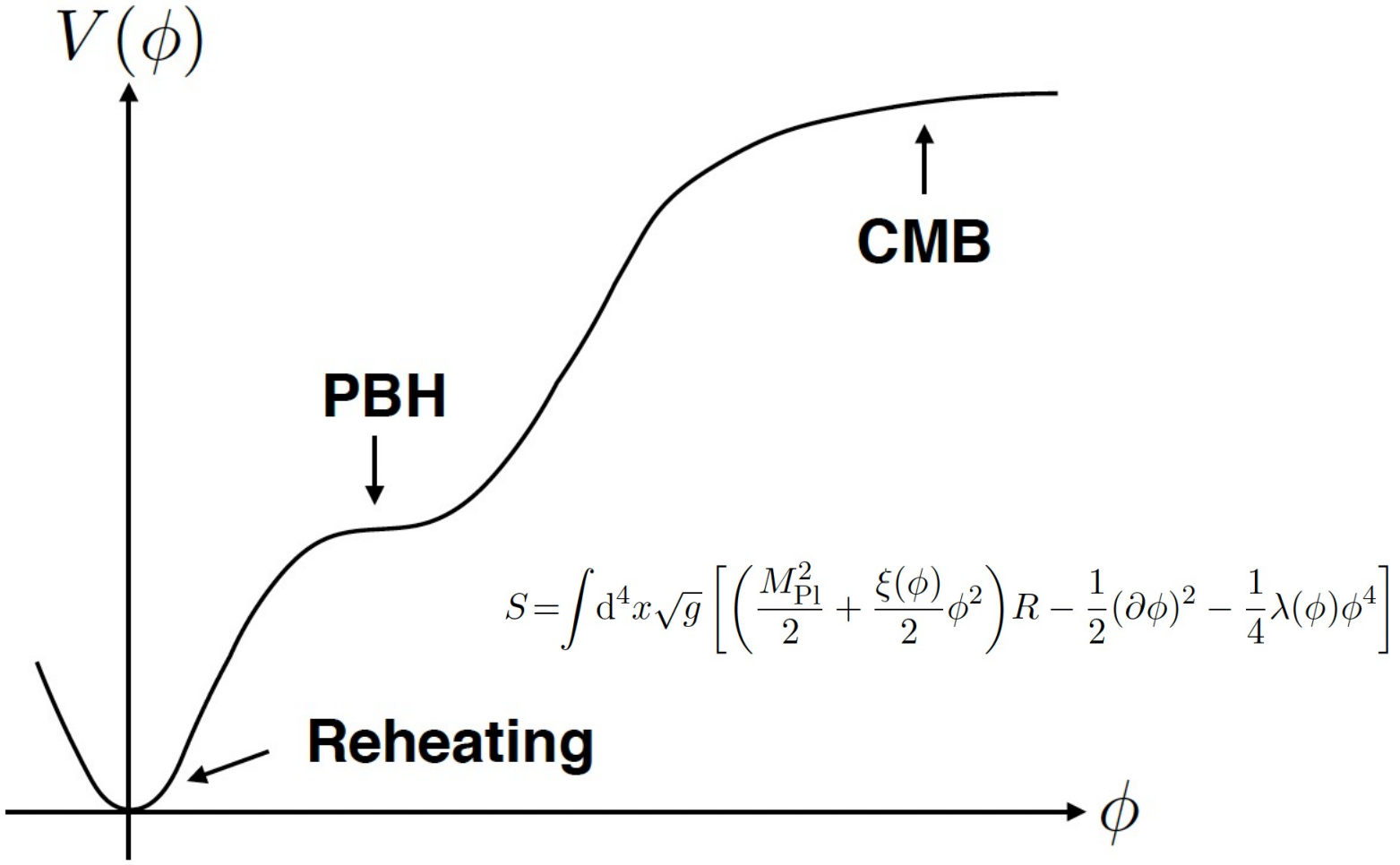

Figure 1. A schematic plot of the inflationary potential with an inflection point.

Primordial Black Hole Review

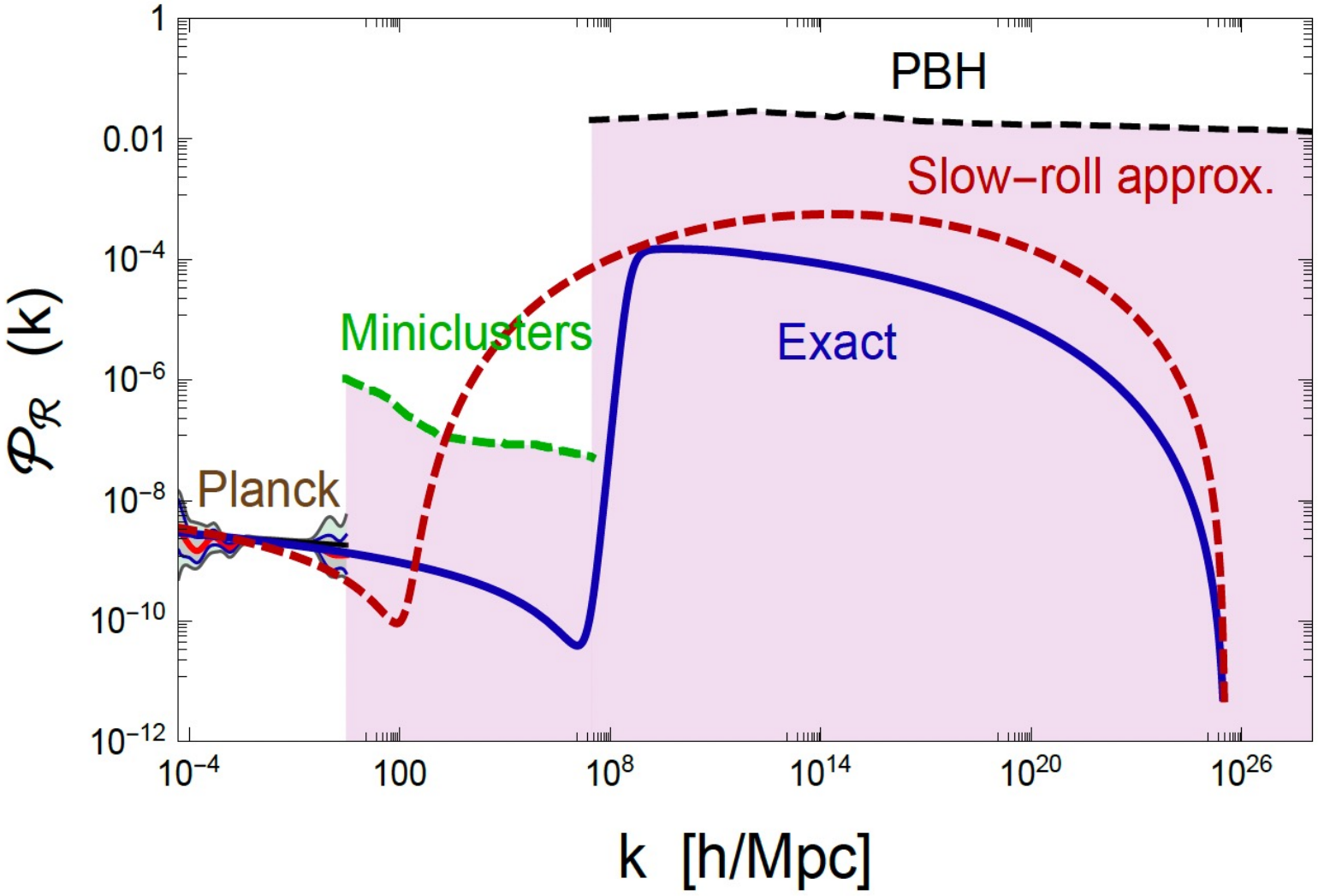

Figure 2. Power spectrum $\mathcal{P}_k$ for the single field Critical Higgs Inflation model, with an inflection point at $N \approx 36$ satisfying the Planck 2018 constraints. Adapted from Ref. [154].

Primordial Black Hole Review

2.1.4 Reverse engineering approach

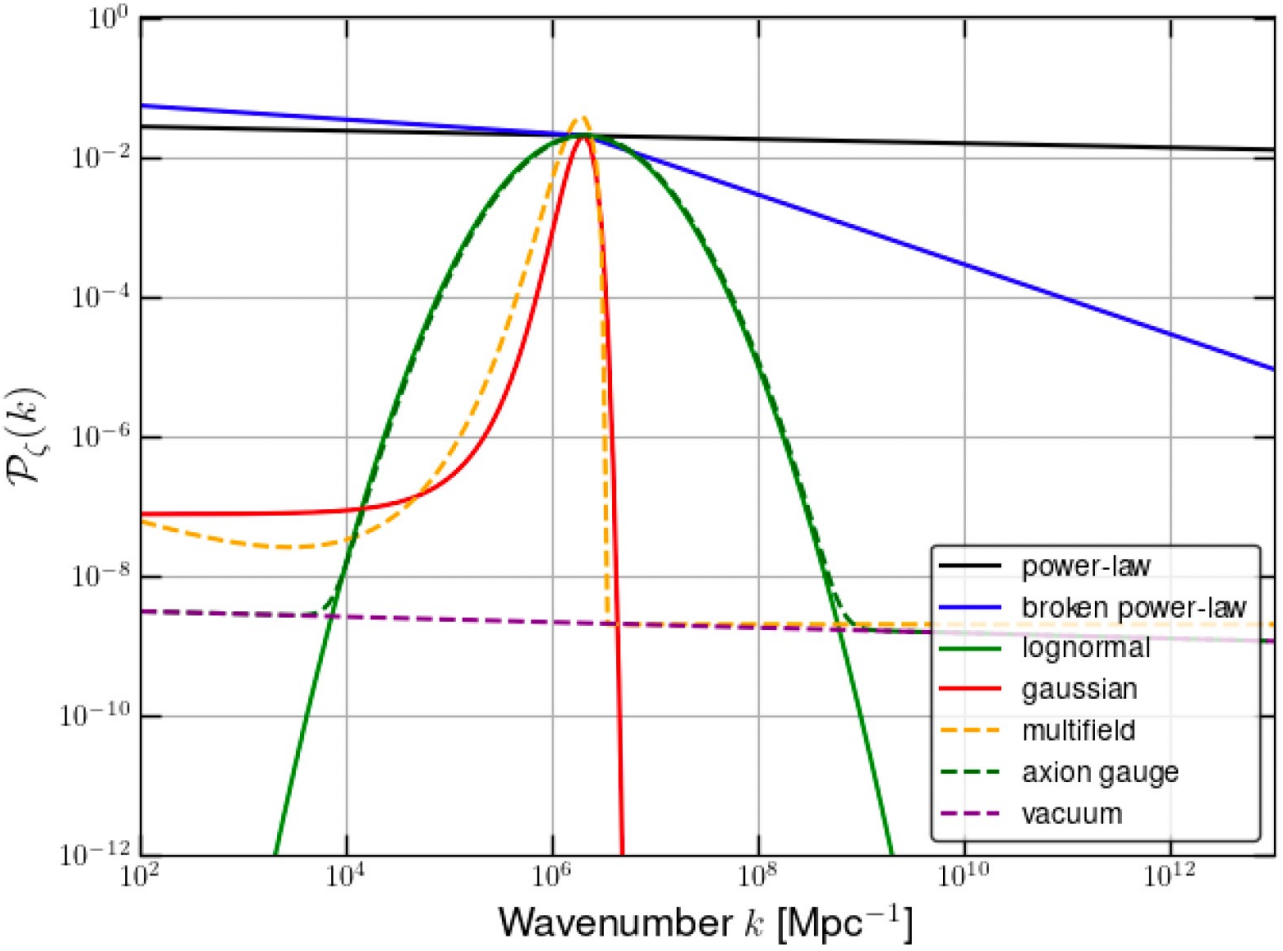

Figure 3. Examples of primordial power spectra of curvature fluctuations, leading to (stellar-mass) PBH formation: power-law, broken power-law, Gaussian and log-normal models (solid lines), and particular examples of multifield and axion-gauge models (dashed lines).

Primordial Black Hole Review

2.2 Multi-field inflationary models

2.2.1 Hybrid inflation

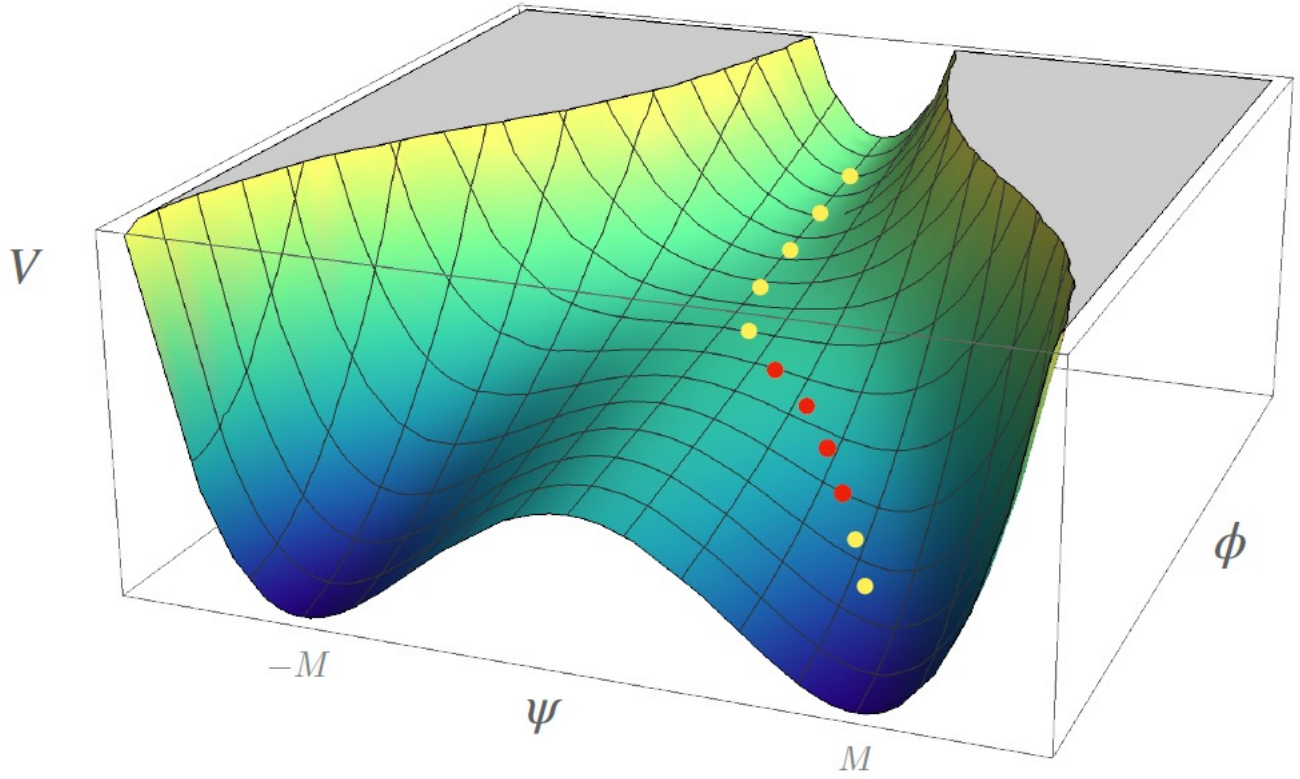

Figure 4. Representation of a typical hybrid inflation potential, V, with a possible trajectory in two-field space (dotted line). CMB perturbations are created along the valley at $\psi = 0$, during a first phase of inflation. Curvature perturbations suitable for production of PBHs are generated in a second flat part of the potential (red dotted line), when the mass-squared of the field ψ changes sign.

Primordial Black Hole Review

2.2.4 Axion-gauge scenario

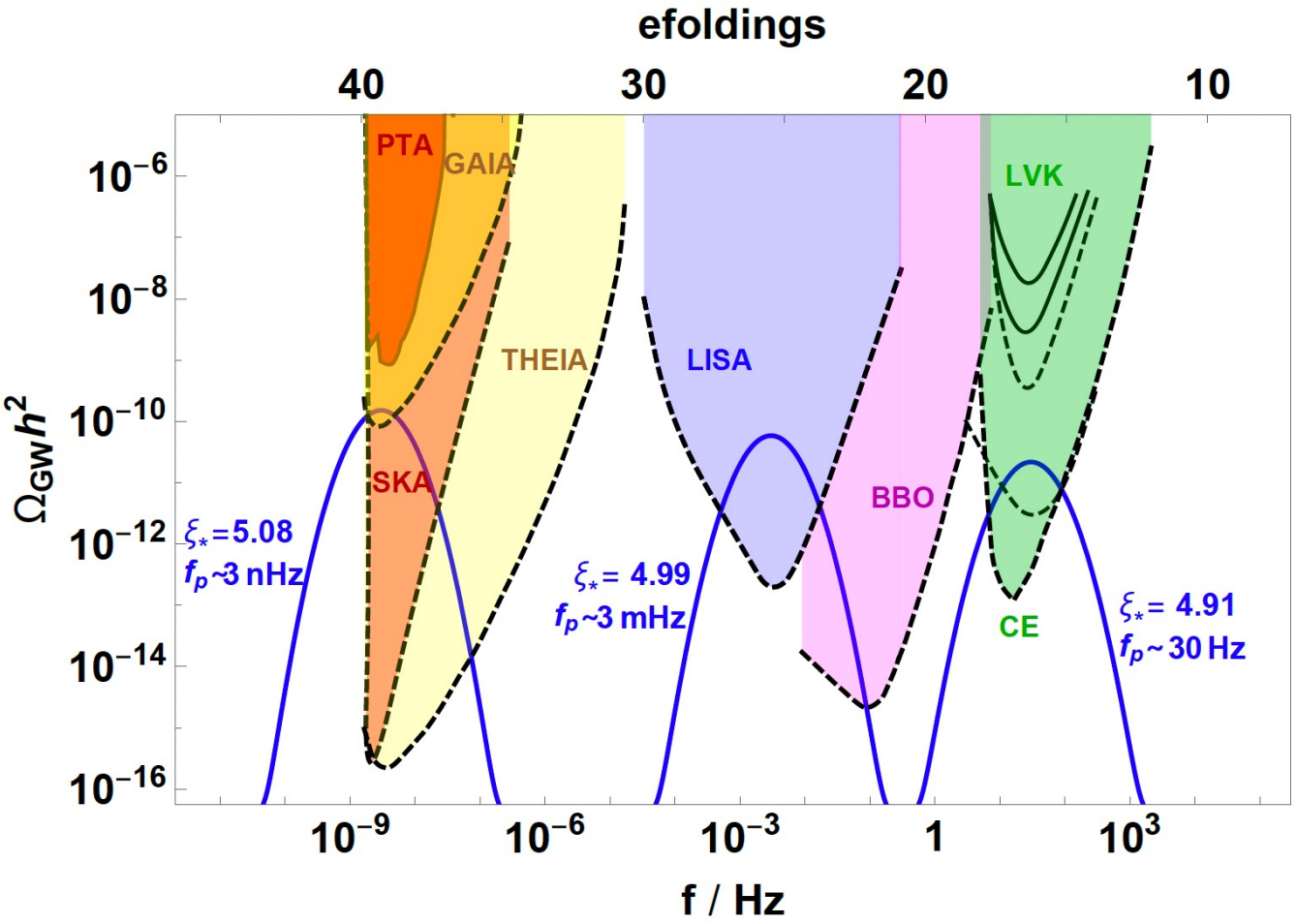

Figure 6. The stochastic GWs produced by axion inflation at four main scales of interferometers, nHz (PTAs and SKA), μHz (Gaia and Theia), mHz (LISA and Taiji) and Hz (LIGO-Virgo-KAGRA (LVK), Einstein Telescope, and Cosmic Explorer). The enhanced density perturbations may produce PBHs which are a significant fraction of dark matter for $1 - 100M_\odot$ and the totality in the $10^{-14} - 10^{-11}M_\odot$

Primordial Black Hole Review

JGB, Papageorgiou, Peloso, Sorbo (2023) [arXiv:2303.13425]

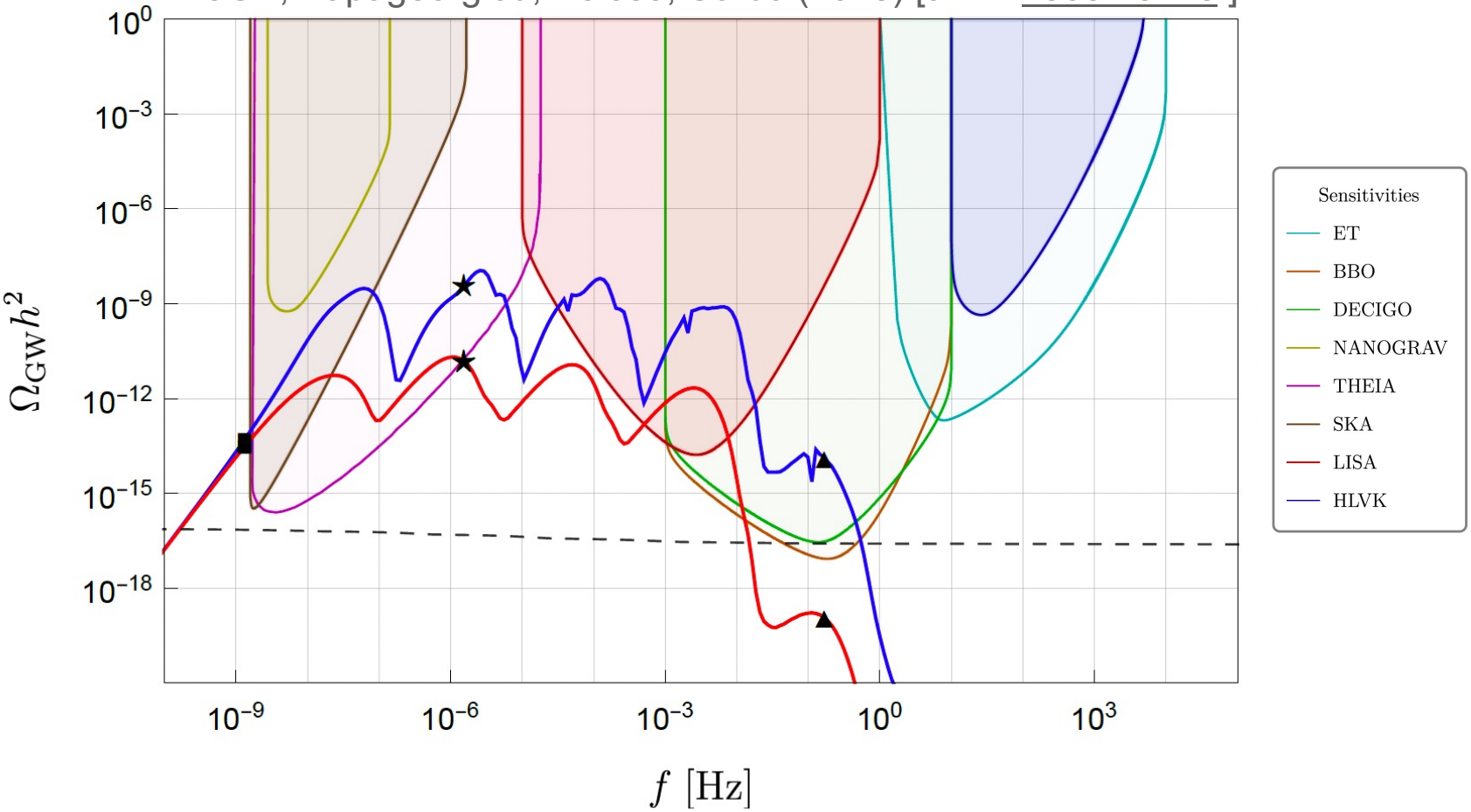

Figure 4. The sourced gravitational wave power spectrum of the *Left* (blue line) and *Right* (red line) polarization as well as the vacuum (back dashed line) superimposed with the power-law-integrated sensitivity curves corresponding to various current and future experiments taken from [39] and [8] in the case of THEIA. The parameters chosen correspond to the coupling strength $1/f = 57/M_p$. The squares, stars and triangles are points for which we plot the integrand of the power spectrum defined in (A.16) in Appendix E.

Primordial Black Hole Review

2.3.2 Quantum diffusion

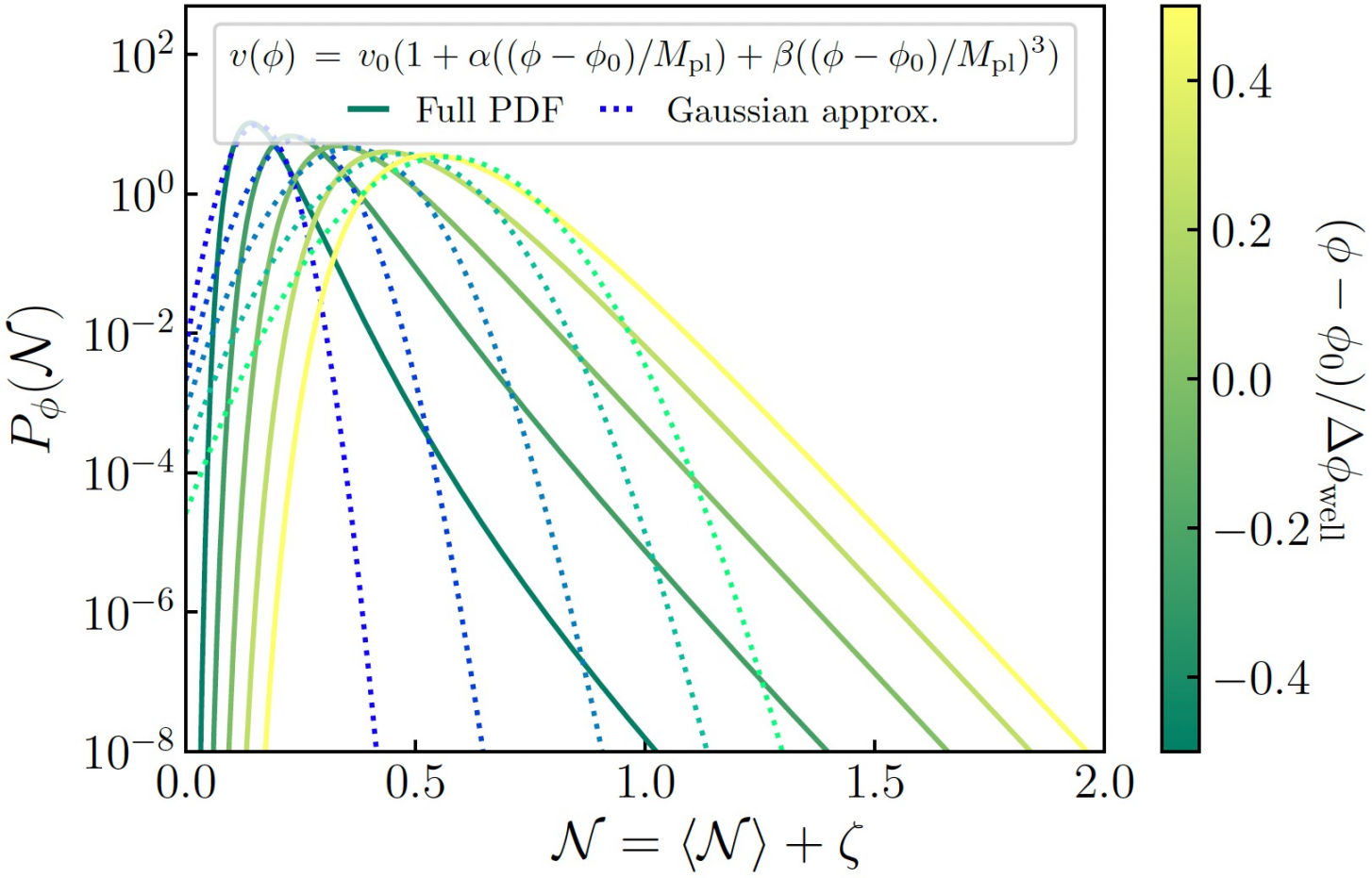

Figure 8. Probability density functions of the curvature perturbations generated by an inflection-point inflationary potential (see inset). Solid lines correspond to the full distribution functions computed by mean of the stochastic-δN formalism, where different colours correspond to different locations in the potential where the scale under consideration emerges from the Hubble radius.

Primordial Black Hole Review

Primordial Black Hole Review

3.8 Thermal history

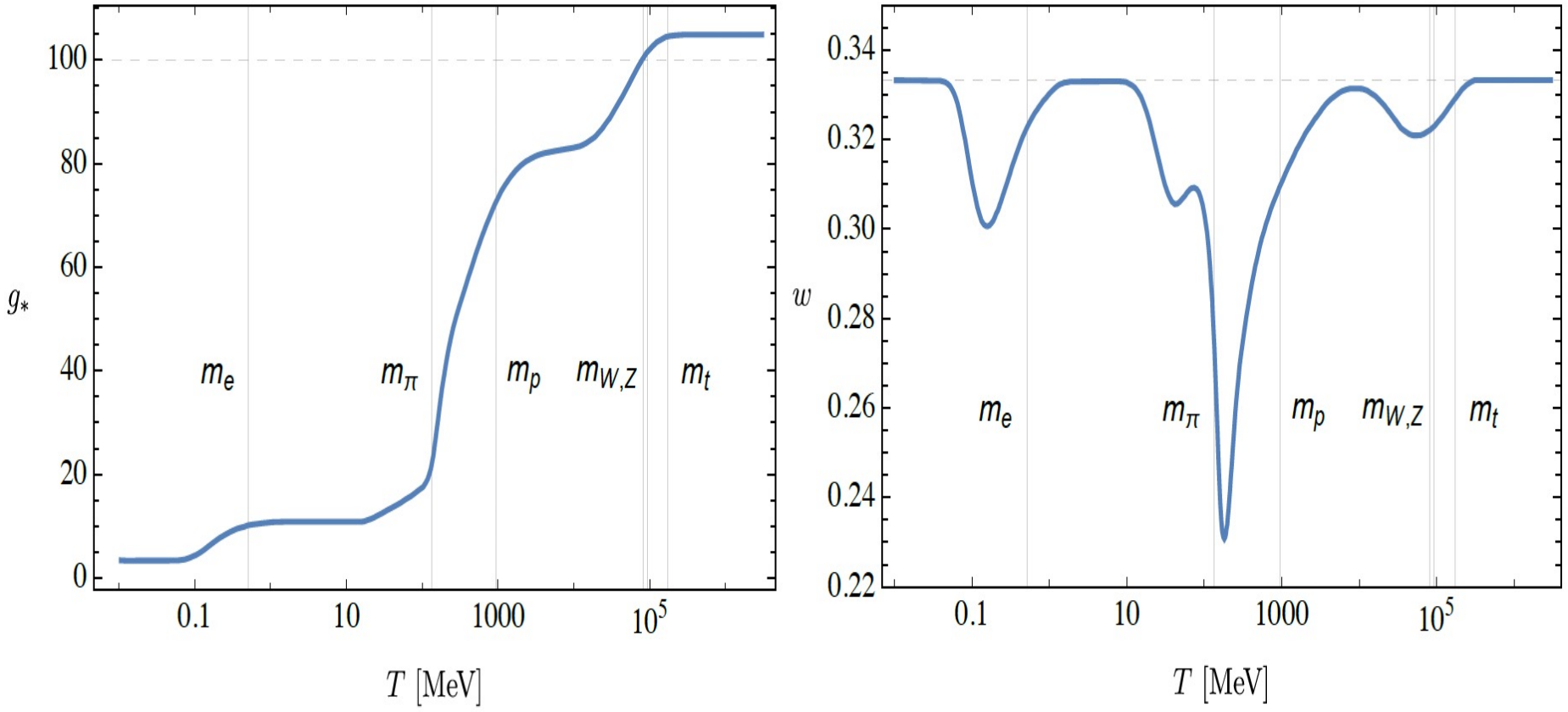

Figure 11. Relativistic degrees of freedom g_* (*Left panel*) and equation-of-state parameter w (*Right panel*), both as a function of temperature T (in MeV). The grey vertical lines correspond to the masses of the electron, pion, proton/neutron, W, Z bosons and top quark, respectively. The grey dashed horizontal lines indicate values of $g_* = 100$ and $w = 1/3$, respectively.

Primordial Black Hole Review

3.3 Threshold for PBH formation

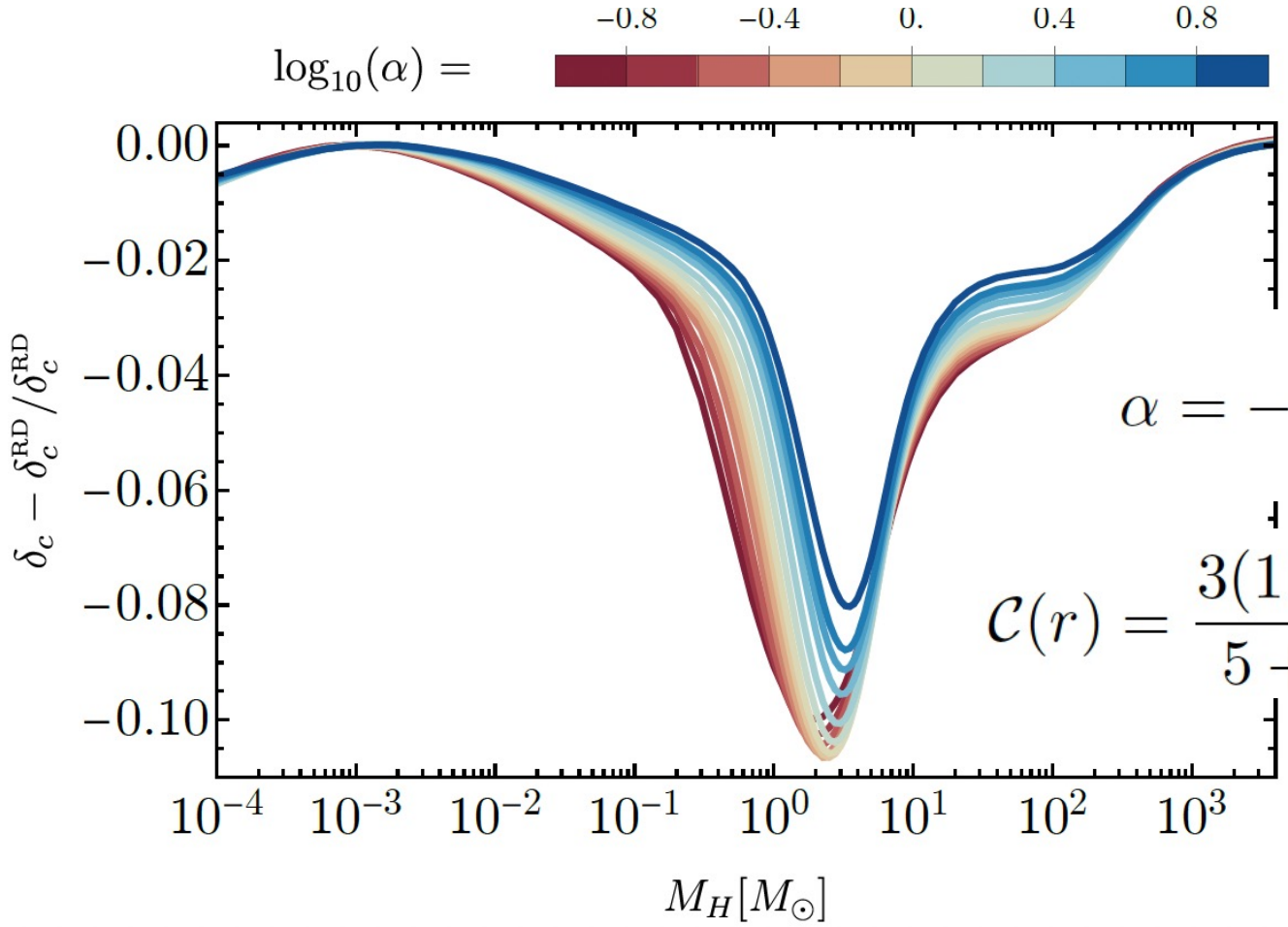

$$\alpha = -\frac{\mathcal{C}''(r_{\rm m})r_{\rm m}^2}{4\mathcal{C}(r_{\rm m})}$$

$$\mathcal{C}(r) = \frac{3(1+w)}{5+3w}K(r)r^2$$

Figure 13. Figure readapted from Ref. [335]. Relative variation of the threshold compared to what is obtained assuming perfect radiation as a function of the horizon crossing time (parametrised here with M_H) induced by the QCD thermal effects. The color code indicates the different values of $\log_{10}(\alpha)$ as indicated by the bar on top of the frame.

Primordial Black Hole Review

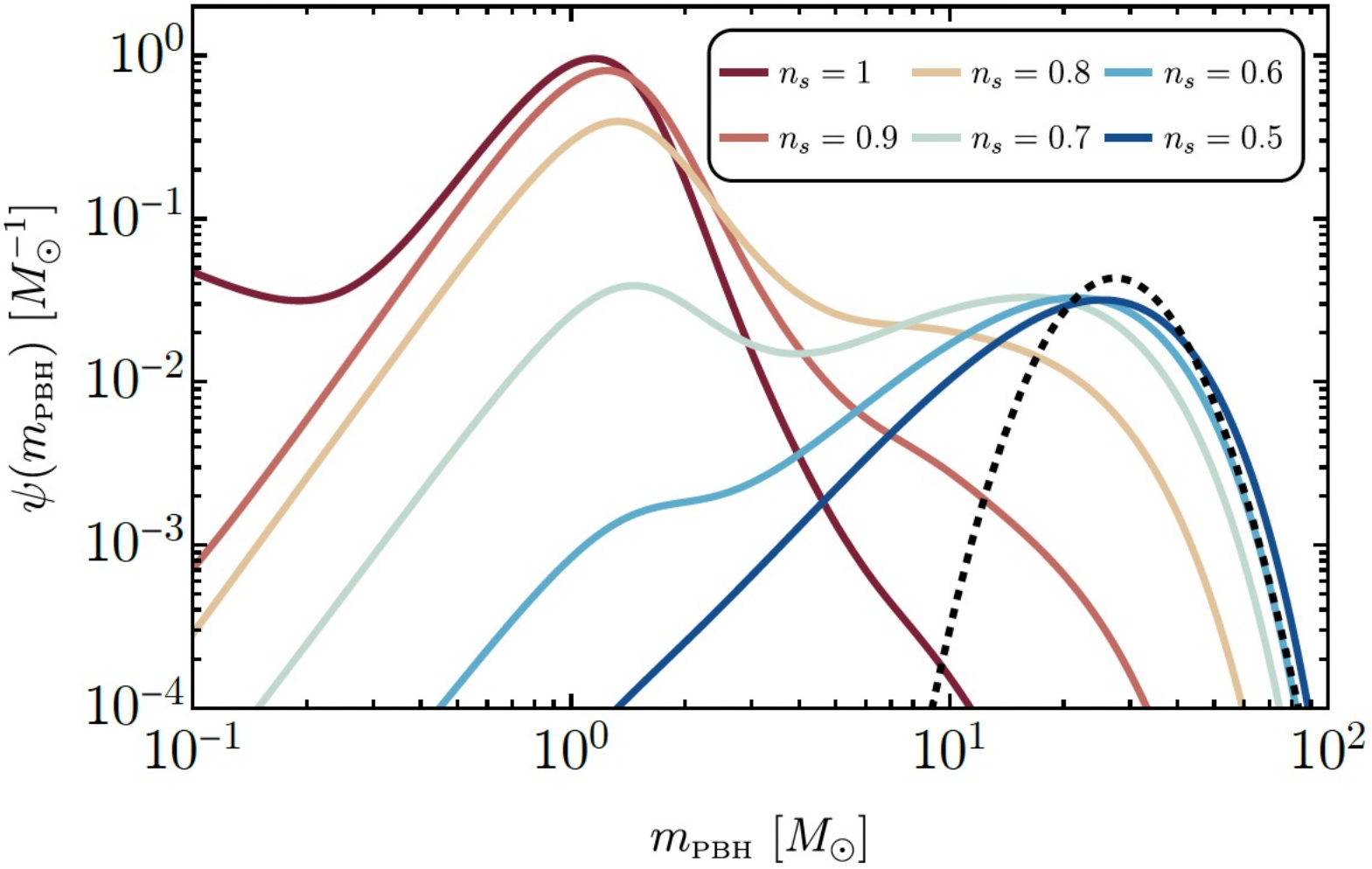

Figure 15. Plot taken from [84]. Mass function obtained with a few choices of the curvature power spectrum. This plot assumes $f_{\rm PBH} = 10^{-3}$, the minimum horizon mass to be $\lesssim 10^{-2.5} M_\odot$, the largest mass $M_H^{\rm max} = 10^{2.8} M_\odot$ and a variable tilt n_s. The black dashed line reports the lognormal mass distribution found as the best fit in the analysis of Ref. [80].

Primordial Black Hole Review

Primordial Black Hole Review

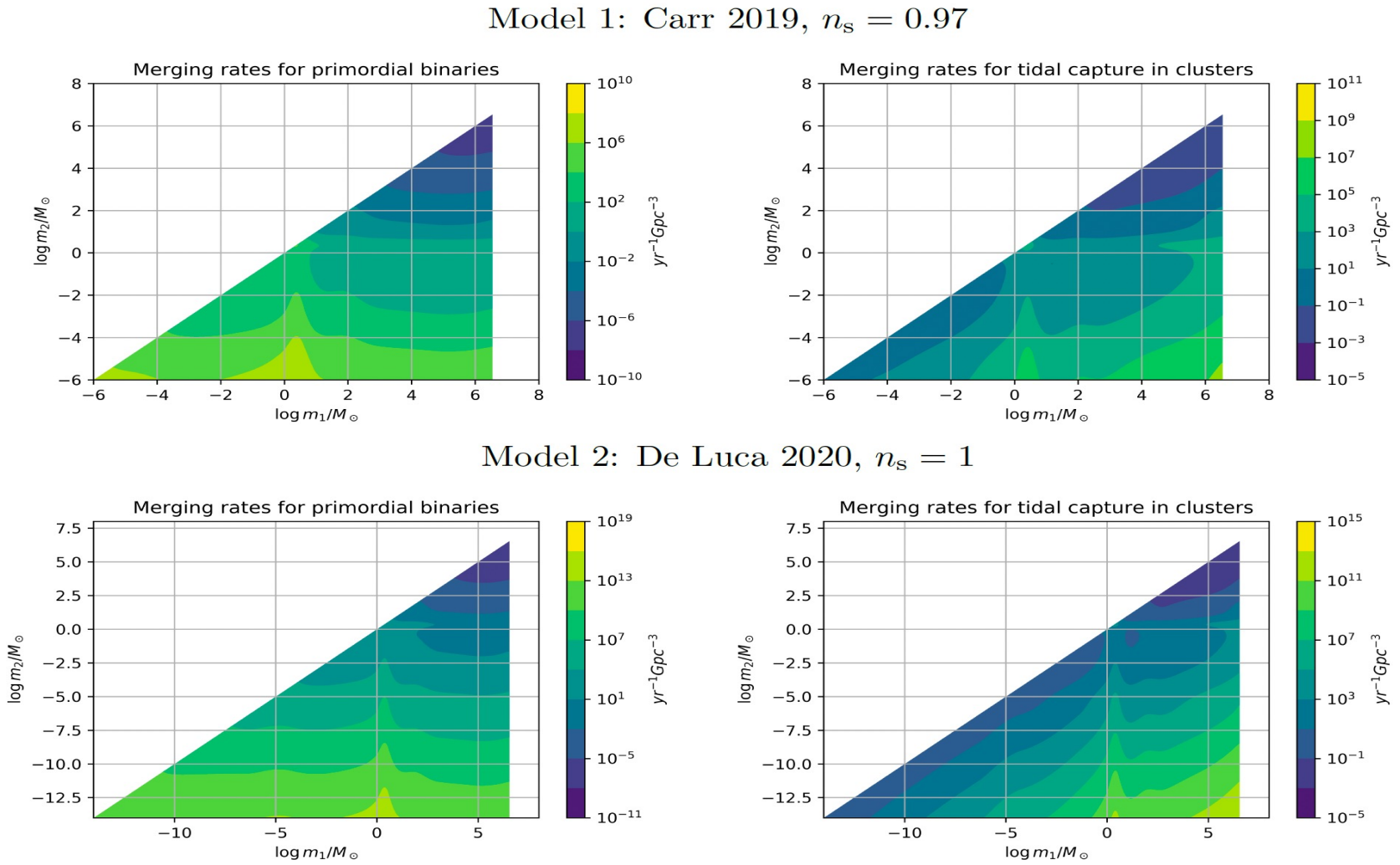

Figure 21. Expected merging rates of PBH of masses m_1 and m_2, for the two mass models represented on Fig. 17 (top panels: Model 1, bottom panels: Model 2), for the two considered binary formation channel: primordial binaries (see Eq. 4.1) on the left panels, and tidal capture in halos (see Eq. 4.11) on the right panels. Figure produced for [359].

Primordial Black Hole Review

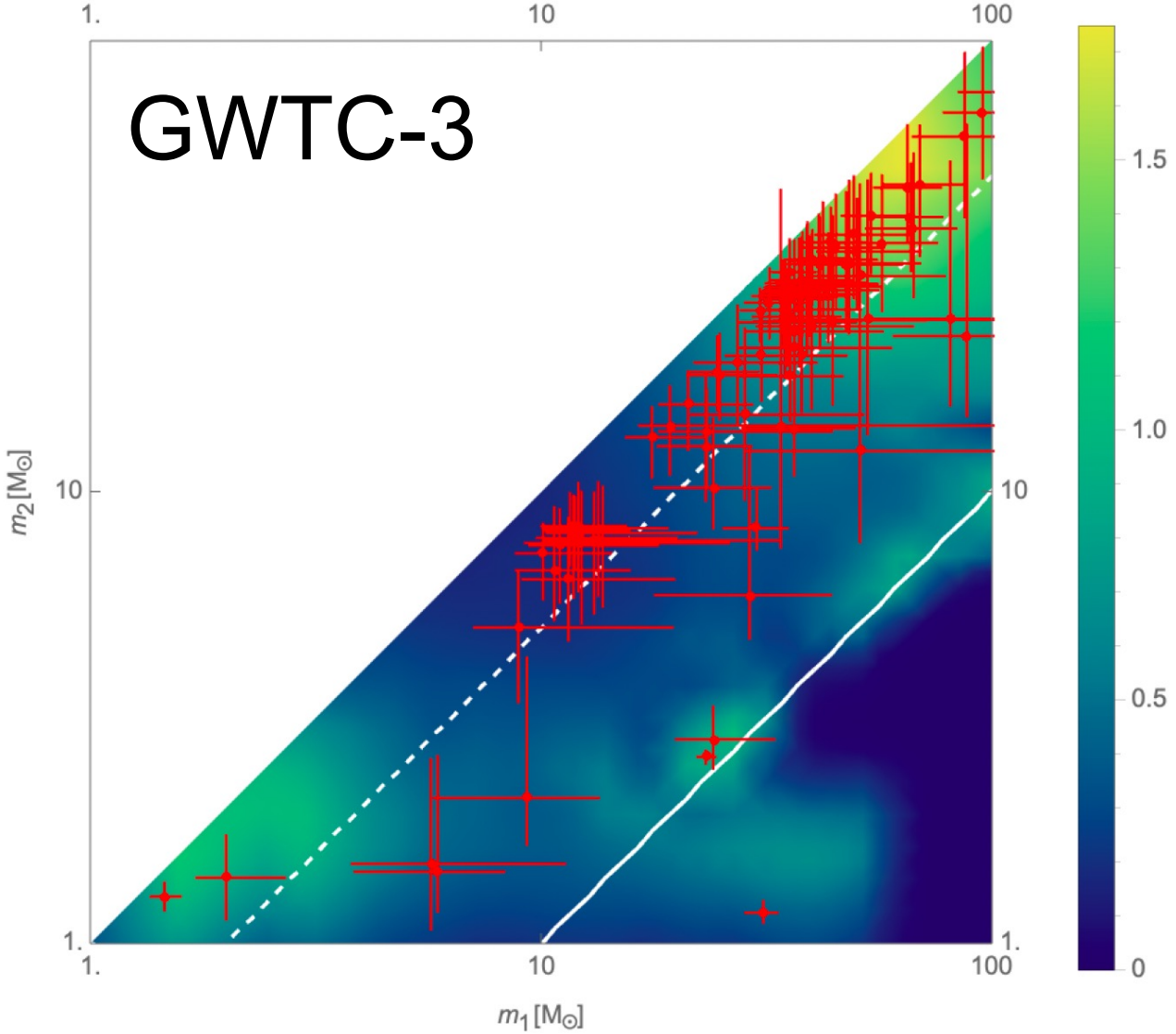

Figure 29. Expected probability distribution of PBH mergers with masses m_1 and m_2 for a mass function with $n_s = 0.97$ and LIGO sensitivity for O3 run. Solid and dashed white lines correspond to mass ratios $q \equiv m_2/m_1$ of 0.1 and 0.5, respectively. From Ref. [215].

Primordial Black Hole Review

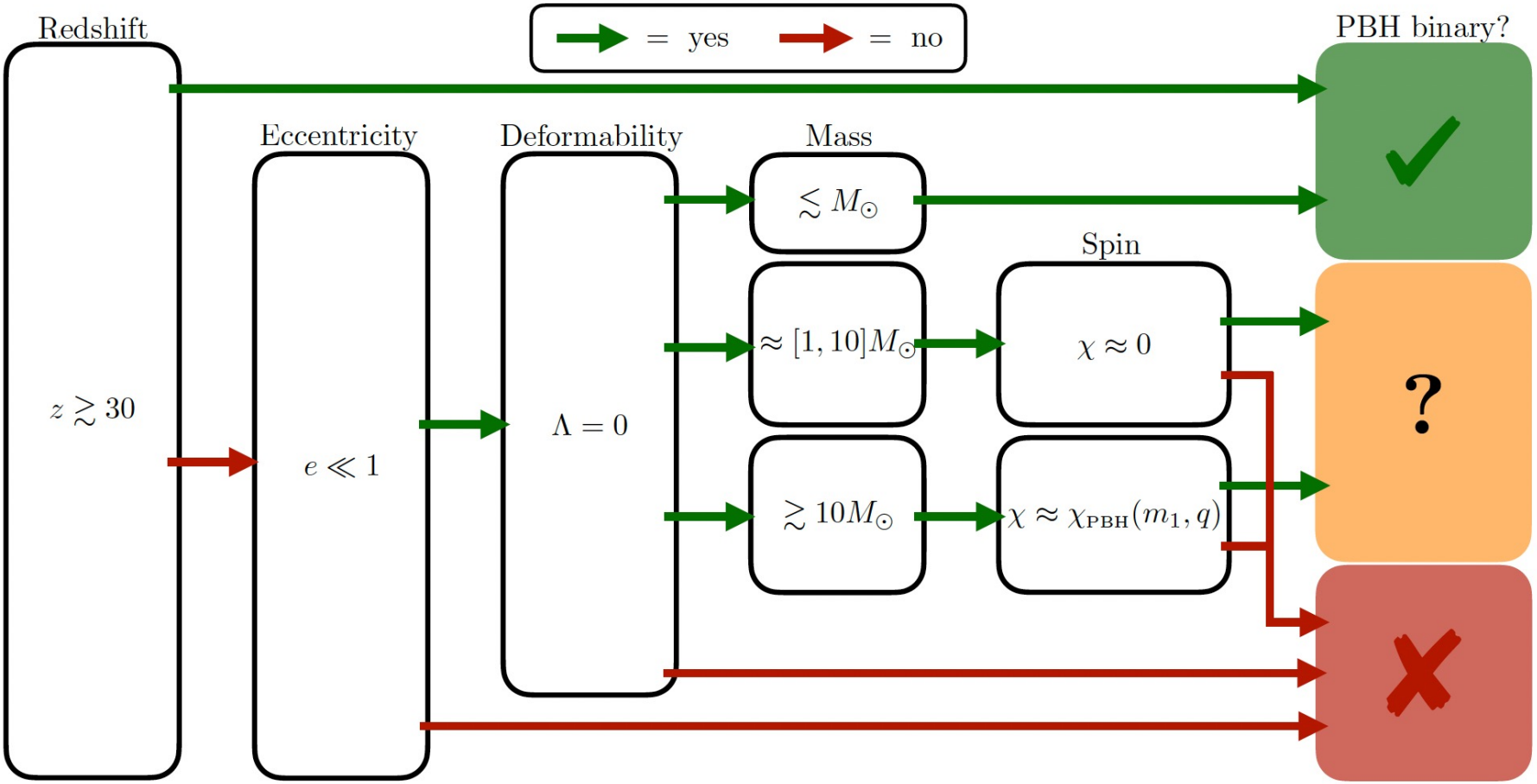

Figure 23. Figure taken from Ref. [82]. Schematic flowchart representing how to systematically rule out or potentially assess the primordial origin of a binary merger. These criteria are based on measurements of the redshift z, eccentricity e, tidal deformability Λ, component masses m, and dimensionless spin χ. Each arrow indicates if the condition in the box is met (green) or violated (red), while the marks indicate: ✓) likely to be a PBH binary; ✗) cannot to be a PBH binary; **?**) may be a PBH binary.

Primordial Black Hole Review

Primordial Black Hole Review

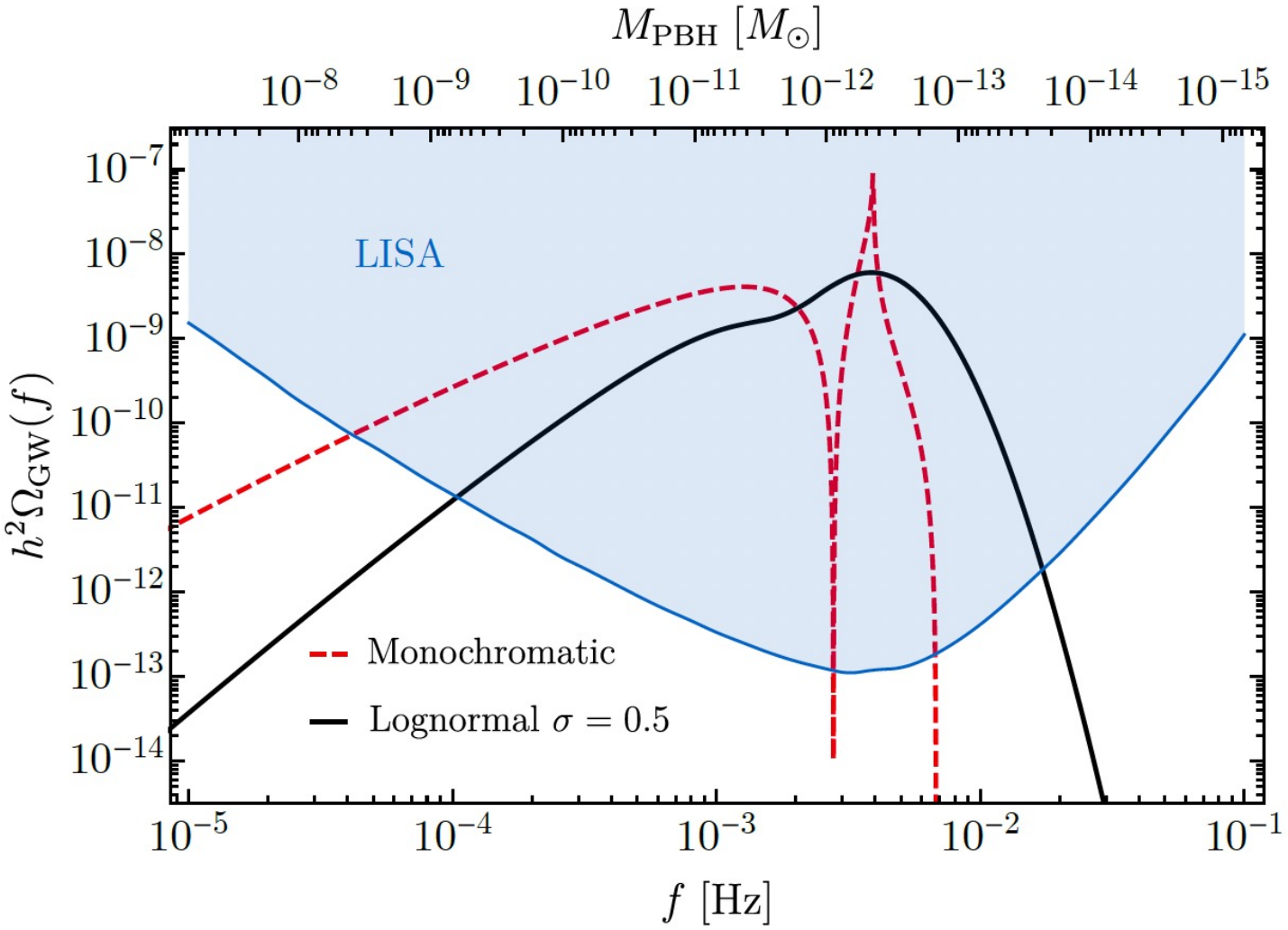

Figure 24. Induced GWs spectra for both examples considered in Eqs. (5.13) and (5.15), for the parameters choice $A_{\rm s} = 0.033$, $A_\zeta = 0.044$ and $\sigma = 0.5$. For comparison, we also show the estimated sensitivity for LISA [92] (the proposed design (4y, 2.5 Gm of length, 6 links) is expected to yield a sensitivity in between the ones dubbed C1 and C2 in Ref. [526]). The PBH mass corresponding to the characteristic frequency is depicted on the top horizontal axis, according to Eq. 5.1.

Primordial Black Hole Review

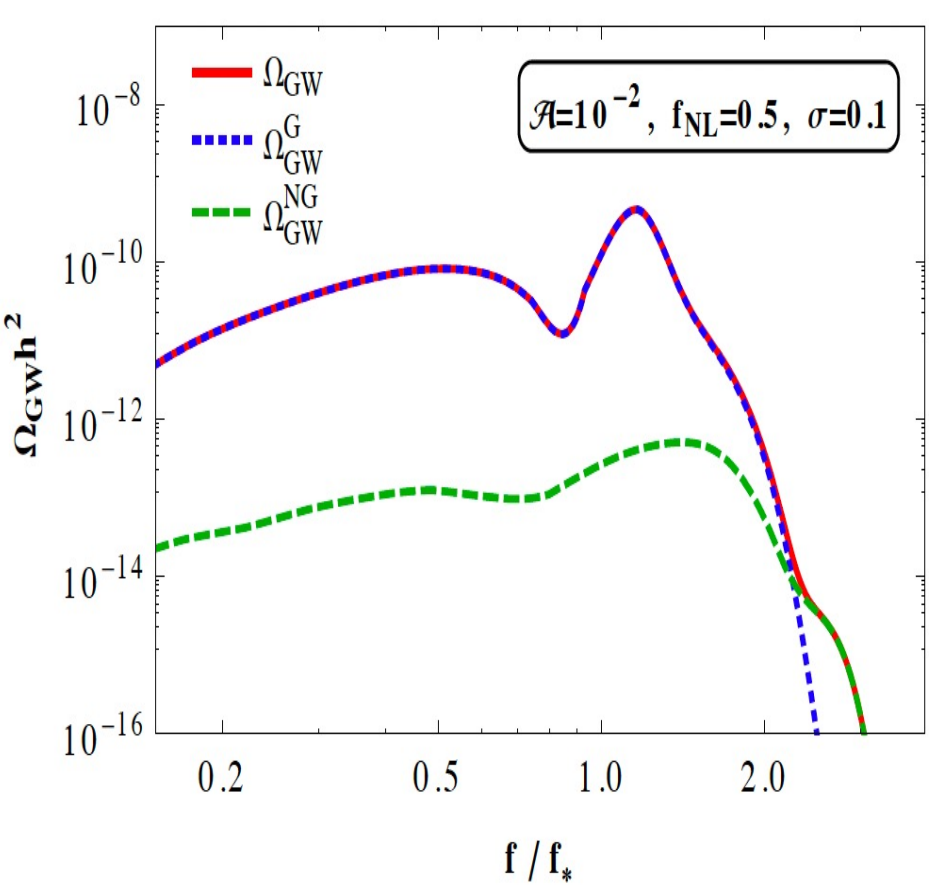

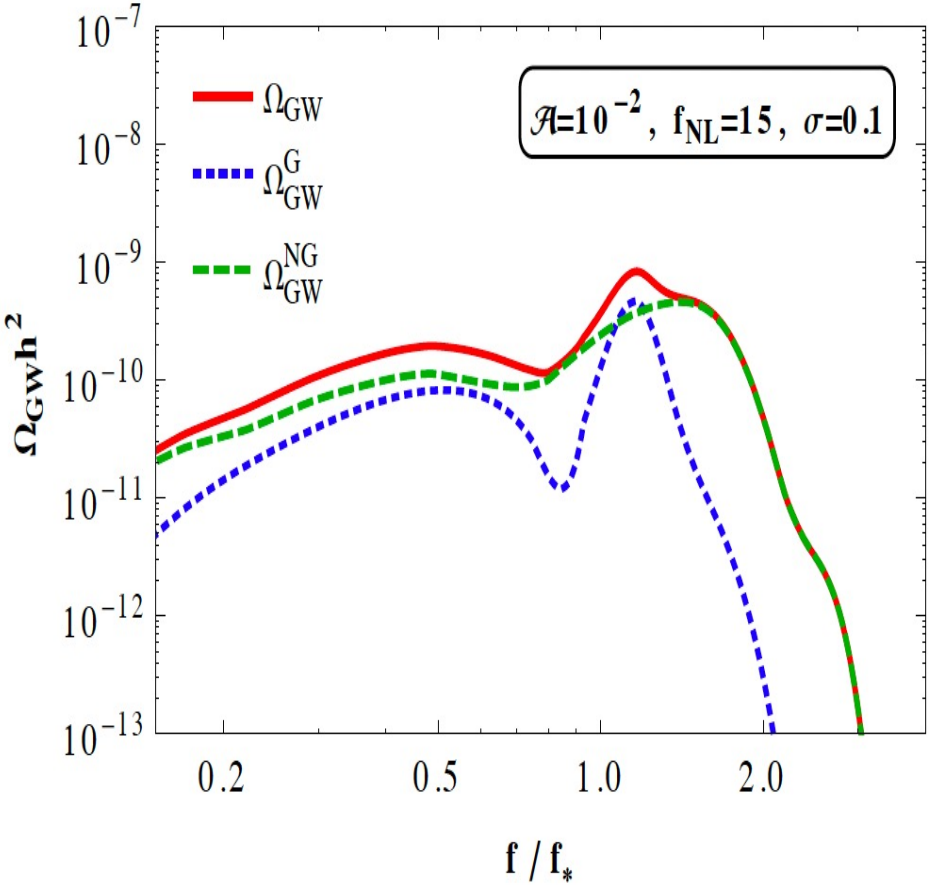

Figure 27. Second peak produced by primordial non-Gaussian component of curvature perturbations. Figure taken from [146].

Primordial Black Hole Review

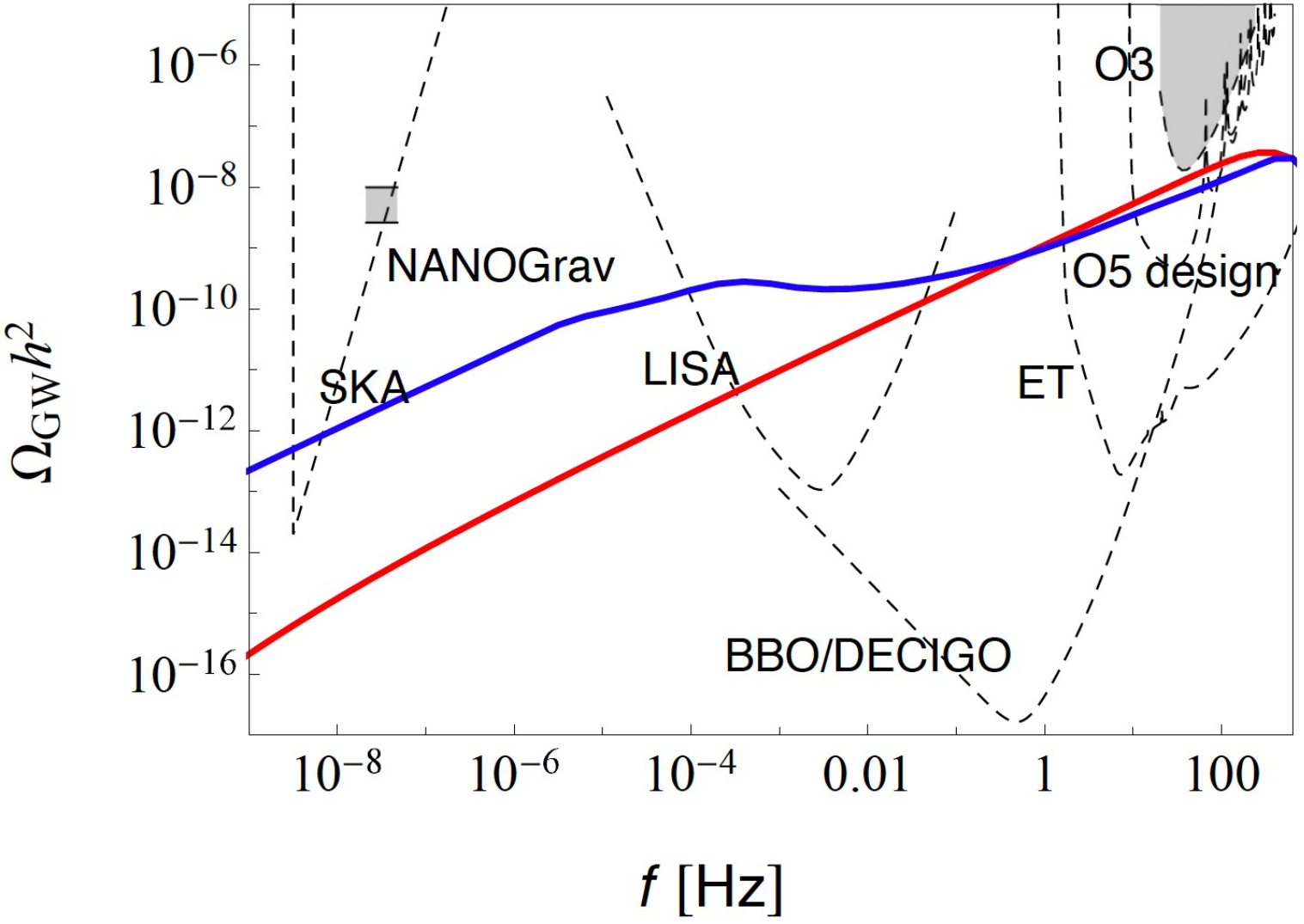

Figure 30. The SGWB spectrum $\Omega_{\rm GW}h^2$ for early PBH binaries with a log-normal mass function (in red, with central mass $\mu = 2.5M_\odot$ and width $\sigma = 1$) and a broad mass distribution with scalar spectral index $n_{\rm s} = 0.970$ (in blue), and $f_{\rm PBH} = 1$.

Primordial Black Hole Review

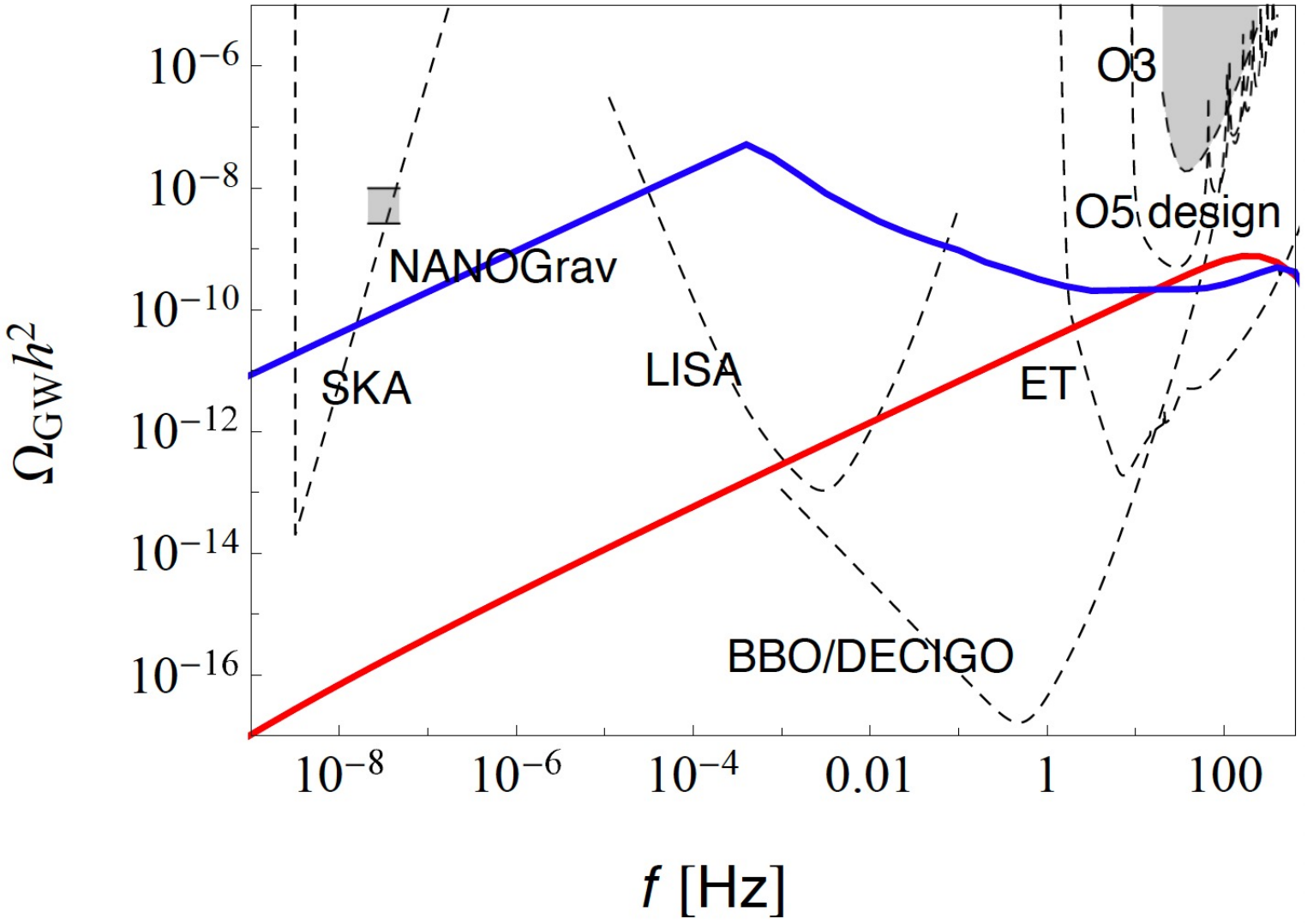

Figure 32. The SGWB spectrum $\Omega_{\rm GW}h^2$ for late PBH binaries in clusters with $f_{\rm PBH} = 1$ for a log-normal mass function (in red, with the central mass $\mu = 2.5M_\odot$ and the width $\sigma = 1$) and a broad mass distribution (in blue, with $n_{\rm s} = 0.97$ and no running).

Primordial Black Hole Review

5.8 From close encounters

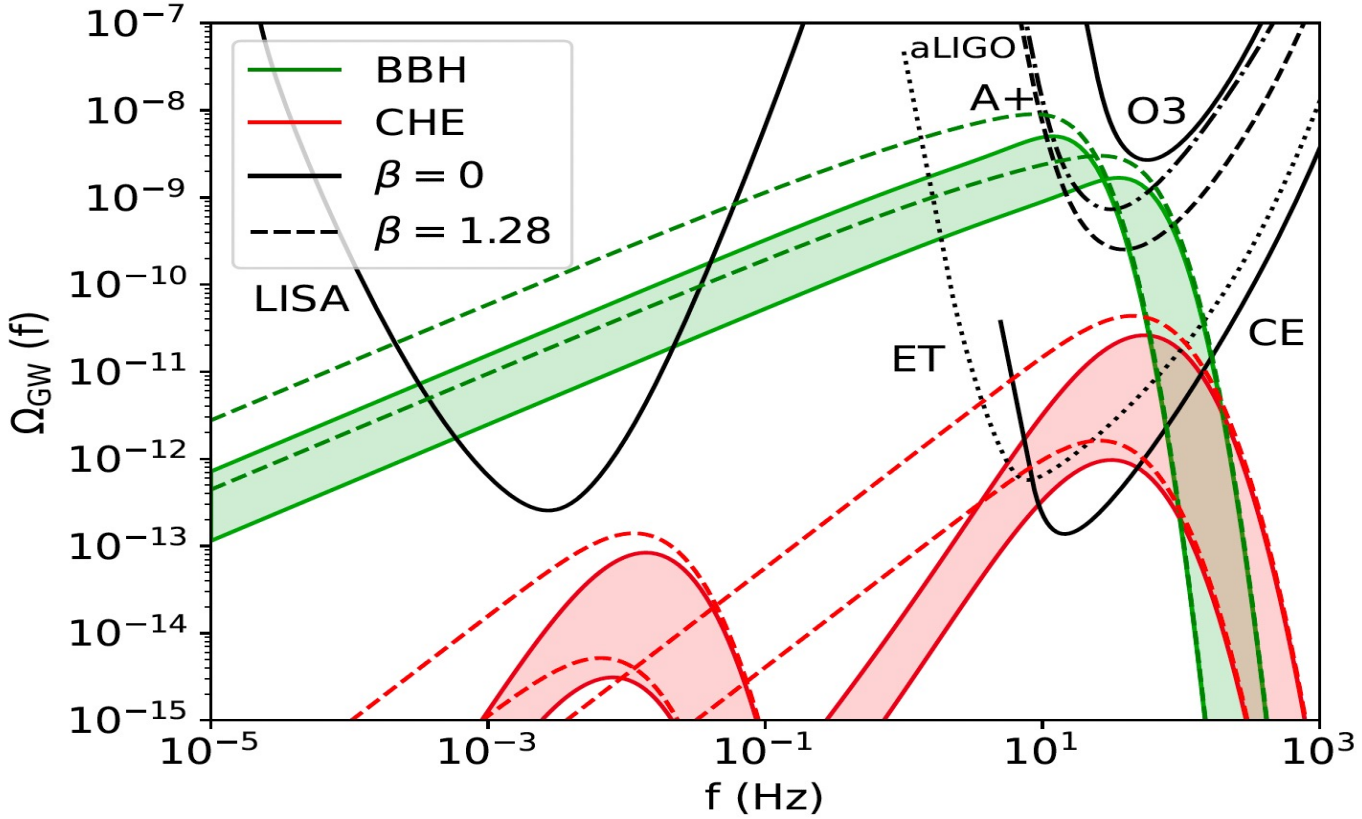

Figure 34. Comparison of the SGWB spectrum originating from BBHs and CHEs, both for $\beta = 0$ (solid) and $\beta = 1.28$ (dashed), where β is a parameter characterizing the redshift dependence of the merger rate as $\tau^{\rm BBH} \propto (1+z)^{\beta}$. For the BBH curves, we take $m_1 = m_2 = 100 - 300\ M_\odot$ and $v_0 = 30$km/s. The CHE curves correspond to the same range of masses with $a_0 = 5$AU, $y_0 = 2 \times 10^{-3}$ for frequencies around 10 Hz, and $a_0 = 5 \cdot 10^7$AU, $y_0 = 10^{-5}$ in the mHz range. For all cases, we assume log-normal distributions for a_0, y_0 and the PBH mass, of respective widths $\sigma_a, \sigma_y = 0.1$, $\sigma_m = 0.5$, as well as $f_{\rm PBH} = 1$. For a smaller fraction of PBHs, the GW spectral amplitude simply scales as $\Omega_{\rm GW} \propto f_{\rm PBH}^2$.

Primordial Black Hole Review

6 GW and LSS correlations

6.1 Introduction

6.2 GW-galaxy cross-correlations for resolved events

6.3 GW-galaxy cross-correlations for the stochastic background

6.4 GW×LSS forecasts

$$\left\langle a^X_{\ell m}(z_i)\, a^{Y*}_{\ell' m'}(z_j)\right\rangle = \delta_{\ell\ell'}\delta_{mm'}\tilde{C}^{XY}_{\ell}(z_i,z_j)$$

$$\widehat{A_{\rm c}} = \frac{\Sigma_\ell \tilde{C}_\ell F_\ell/{\rm Var}[\tilde{C}_\ell]}{\Sigma_\ell F_\ell^2/{\rm Var}[\tilde{C}_\ell]}$$

$$F_\ell \equiv d\tilde{C}_\ell/d\widehat{A_{\rm c}}$$

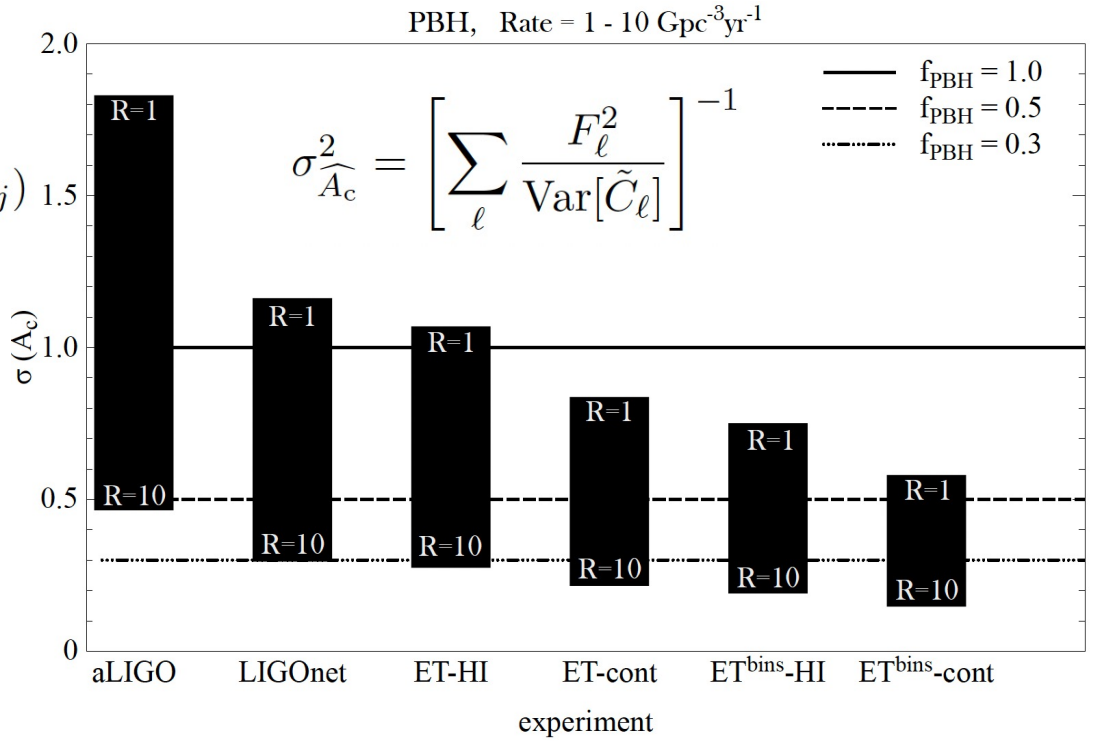

Figure 35. Forecast errors on the cross-correlation amplitude, $A_{\rm c}$, for different experiment combinations, varying merger rates and years of observations. Each column corresponds to a GW detector experiment, for merger rates from 1 to 10 Gpc^{-3}yr^{-1}. Horizontal lines show the expected difference in the cross-correlation between (late binary) PBH and stellar binaries, for different values of $f_{\rm PBH}$.

Primordial Black Hole Review

Primordial Black Hole Review

Primordial Black Hole Review

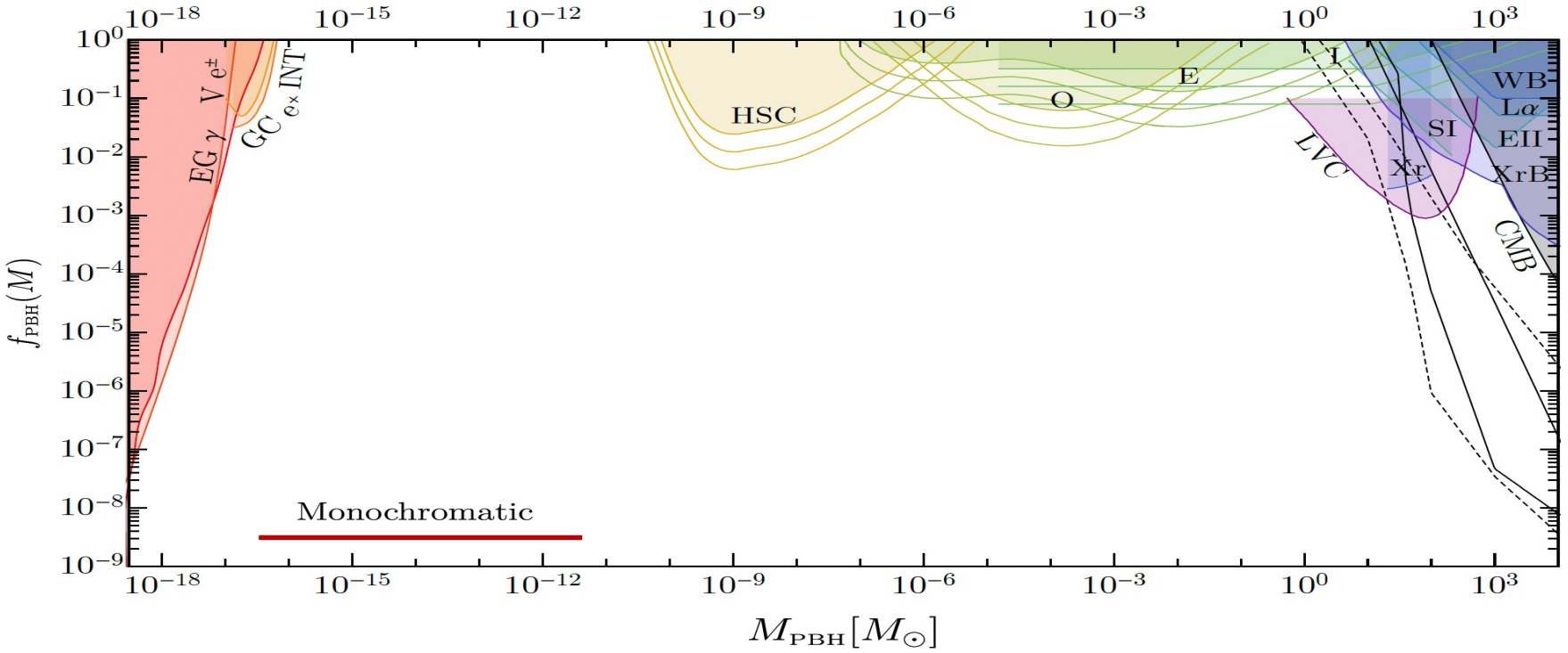

Figure 39. We show the most stringent claimed constraints in the mass range of phenomenological interest. They come from the Hawking evaporation producing extra-galactic gamma-ray (EG γ) [627], $e^{\pm}$ observations by Voyager 1 (V $e^{\pm}$) [628], positron annihilations in the Galactic Center (GC e^{+}) [629] and gamma-ray observations by INTEGRAL (INT) [630] (for other constraints in the ultra-light mass range see also [143, 631–635]). We plot microlensing searches by Subaru HSC [110, 113], MACHO/EROS (E) [636, 637], Ogle (O) [114] and Icarus (I) [638]. Other constraints come from CMB distortions. In black dashed, we show the ones assuming disk accretion (Planck D in Ref. [372] and Ref. [639], from left to right) while in black solid the ones assuming spherical accretion (Planck S in Ref. [372] and both photo- and collisional ionization in Ref. [100], from left to right). Only Ref. [372] includes the effect of the secondary dark matter halo in catalysing accretion. Additionally, constraints coming from X-rays (Xr) [640] and X-Ray binaries (XrB)[641] are shown. Dynamical limits coming from the disruption of wide binaries (WB) [642], survival of star clusters in Eridanus II (EII) [106] and Segue I (SI) [643, 644] are also shown. LVC stands for the constraint coming from LIGO/Virgo Collaboration measurements [62, 78, 377, 408]. Constraints from Lyman-α forest observations (Lα) come from Ref. [645]. We neglect the role of accretion which has been shown to affect constraints on masses larger than $\mathcal{O}(10)M_\odot$ [77, 371] in a redshift dependent manner. See Ref. [65] for a comprehensive review on constraints on the PBH abundance. Notice that there are no stringent bounds in the asteroid mass range [646, 647] where LISA may constrain PBHs through the search of a second order SGWB.

Primordial Black Hole Review

Carr, Clesse, JGB, Hawkins, Kuhnel (2023)

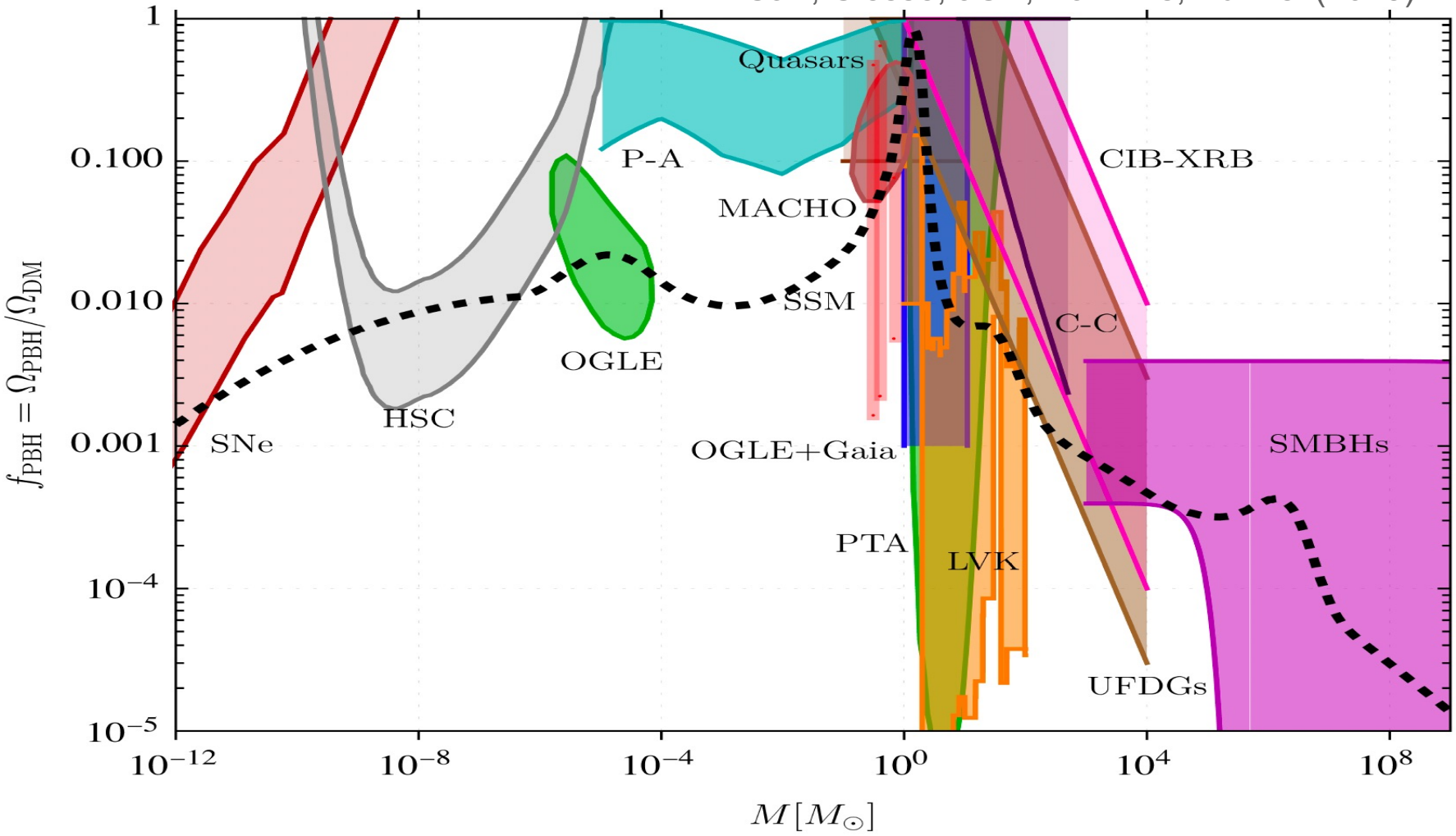

Figure 1. Summary of positive evidence for PBHs in terms of $f_{\rm PBH}$ values required by or consistent with the claimed detections. These come from PBH-attributed signals from supernovæ (SNe), various microlensing surveys (Gaia, HSC, OGLE, MACHO), pixel-lensing (P-A), gravitational waves (LVK), ultra-faint dwarf galaxies (UFDGs), supermassive black holes (SMBHs), core/cusp (C-C) profiles for inner galactic halos, and correlations of the source-subtracted cosmic infrared and X-ray backgrounds (CIB-XRB).

Primordial Black Hole Review

Primordial Black Hole Review

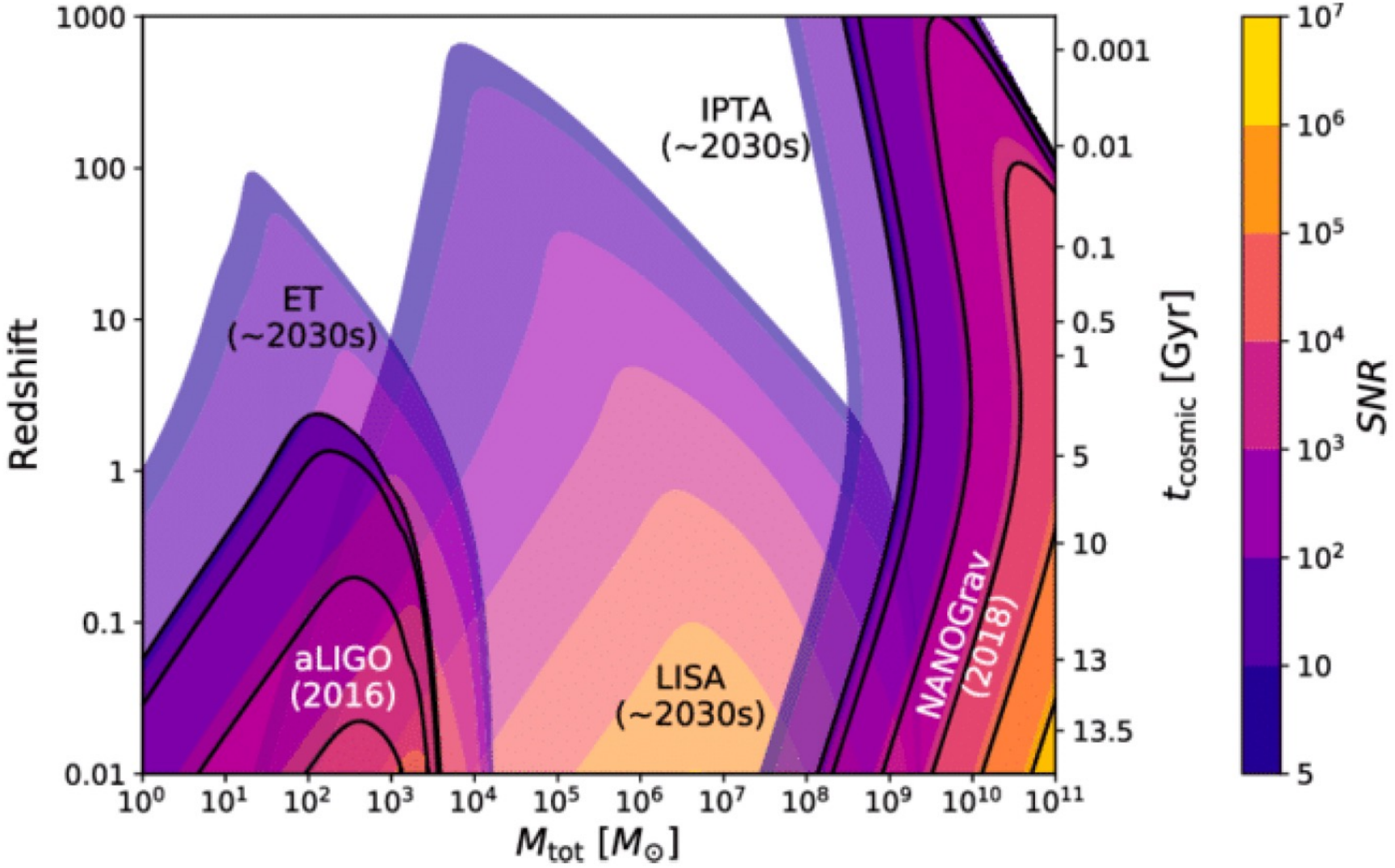

Figure 44. Redshift range of LISA for equal-mass BBH coalescences as a function of the total system mass and comparison with the range of other detectors and pulsar timing arrays. The color scale represents the expected SNR.

Primordial Black Hole Review

9 Conclusions

One important conclusion of our analysis of the recent literature on PBHs is that strong claims, in one or another direction, are certainly premature and generally rely on hypotheses that are very hard to test. Thus, there is still a huge amount of work to be done before making precise predictions. We therefore encourage others to pursue this direction and hope that our work will provide motivation and tools for researchers from other fields to join the growing PBH community.

Future

Our work will soon be accompanied by a numerical code to compute all these gravitational-wave observations, for a wide variety of models. This code is currently under development and testing, but some of our key figures were already produced using it. This is a first promising perspective of this work. Then, our review also sheds light on the physical processes that are still subject of large uncertainties, like the role of PBH accretion and clustering, or the PBH binary disruption. We also discuss the fact that all signatures are highly model dependent.